https://doi.org/10.5194/egusphere-2026-2150
Preprint. Discussion started: 27 May 2026

Accurate assessment of surface mass balance based on stake observations and model correction at Dome A, East Antarctica

Xiyue Zhang[1], Minghu Ding[1,2], Diyi Yang[1,3], Bin Cheng[4], Ian Allison[5], Kongju Zhu[1], Yuande Yang[6,7], Xiangbin Cui[8], Petra Heil[9], Chuanjin Li[8], Cunde Xiao[10]

[1]State Key Laboratory of Disaster Weather Science and Technology, Chinese Academy of Meteorological Sciences, Beijing 100081, China
[2]Key Laboratory of Polar Atmosphere-Ocean-Ice System for Weather and Climate, Ministry of Education, Shanghai 200438, China
[3]Haining Meteorological Bureau, Haining 314400, China
[4]Finnish Meteorological Institute, Helsinki, Finland
[5]Institute for Marine and Antarctic Studies, University of Tasmania, Hobart, Australia
[6]Chinese Antarctic Center of Surveying and Mapping, Wuhan University, Wuhan 430079, China
[7]Key Laboratory of Polar Environment Monitoring and Public Governance, Ministry of Education, Wuhan University, Wuhan 430079, China
[8]Antarctic Zhongshan Ice and Space Environment National Observation and Research Station, Polar Research Institute of China, Shanghai 201209, China
[9]Australian Antarctic Division and Australian Antarctic Program Partnership, University of Tasmania, Hobart, Australia
[10]State Key Laboratory of Earth Surface Processes and Resource Ecology, Beijing Normal University, Beijing 100875, China

Correspondence to: Minghu Ding (dingminghu@foxmail.com)

Abstract. Accurate quantification of surface mass balance (SMB) in the Antarctic interior underpins ice sheet mass budget assessments and ice core interpretation. Stake measurements, however, systematically underestimate SMB because firn densification causes surface lowering unrelated to mass change. Here, we simulate firn compaction with a firn densification model and correct stake records from 2008-2024 at Dome Argus (Dome A), East Antarctica, thereby refining SMB estimates and their spatial variability. The mean annual corrected SMB is 24.14 kg $m^{-2}yr^{-1}$, 8.8 % higher than the uncorrected value (22.19 kg $m^{-2}yr^{-1}$). Over the stake array, the RACMO2.4p1 regional model yields lower and more spatially uniform SMB (17.50 kg $m^{-2}yr^{-1}$). Using automatic weather station observations, we estimate annual sublimation of 2.34 mm w.e. yr^{-1} and hoar deposition of 0.87 mm w.e. yr^{-1}, indicating that the net vapor flux is equivalent to 5.7 % of the total mass input. This framework reduces densification induced bias in stake-derived SMB, provides an observational benchmark for evaluating regional climate models, and supports accurate dating of ice core climate records from Dome A.

Keywords: Firn compaction model; surface mass balance; stake method; sublimation; East Antarctic; Dome Argus

1 Introduction

As the largest freshwater reservoir on earth, the Antarctic Ice Sheet (AIS) plays a decisive role in global sea-level rise through its mass variations, and its complete melting would contribute significantly to global sea-level rise (Pritchard et al., 2025;

https://doi.org/10.5194/egusphere-2026-2150
Preprint. Discussion started: 27 May 2026

Rignot et al., 2019). Recent assessments indicate that the AIS has been losing mass at an accelerating rate, with the estimated loss around 131 Gt yr^{-1} (Diener et al., 2021). Dome Argus (Dome A), the highest region of the East Antarctic Ice Sheet, is characterized by low temperature and low accumulation rate, representing the extreme climate conditions of the Antarctic interior. These conditions result in well-preserved stratigraphic layers in ice cores, which facilitates chronological reconstruction and make Dome A a good site for deep ice core drilling (Xiao et al., 2008a; Cui et al., 2010). Surface mass balance (SMB), which comprises the net gain from snowfall less loss from sublimation/erosion, plays a significant role in the mass balance of the AIS and hence global sea-level projections (Lenaerts et al., 2019). Accurate evaluation of the SMB is a prerequisite for understanding the mass budget and for interpreting deep ice core records. This is particularly important at Dome A, where deep ice core drilling is a major scientific objective. However, due to the extreme environment at Dome A, reliable SMB quantification remains challenging.

The Regional Atmosphere Climate Model (RACMO) can provide large-scale estimations of SMB, but the paucity of ground-based observations across the Antarctic interior requires in situ measurements to ensure reliable SMB (Mottram et al., 2021; Van Wessem et al., 2018; Van Dalum et al., 2025). The classic stake method has been widely applied for measuring SMB because of its simplicity, durability and low cost (Eisen et al., 2008). The principle of the stake method is to insert a stake into the snow and record temporal changes in distance between the surface and the top of the stake, thereby obtaining surface height variations (Ding et al., 2015; Kameda et al., 2008). In order to estimate SMB over Dome A, the Chinese National Antarctic Research Expedition (CHINARE) established stake farms. During the period 2008-2013, stake array measurements indicated an SMB of 22.9 $kg\,m^{-2}yr^{-1}$ (Ding et al., 2016). However, a key limitation of the stake method is its sensitivity to firn densification. The entire firn snow layer is constantly compressing under the influence of temperature and overburden pressure. This means that the change of snow height is due not only to the accumulation of new snow but also to the compaction of firn snow layers (Li & Zwally, 2011; Smith et al., 2023). This leads to a systematic underestimation of SMB, particularly in low accumulation areas such as Dome A.

Therefore, SMB derived from stake measurements must be corrected for firn densification effects. For example, at Vostok, Ekaykin et al. (2020) estimated the densification-induced height reduction using two methods. One method was based on Sorge's law (Sorge, 1935) combined with measured density profiles to calculate the densification contribution, while the second method was based on direct field measurements of the compaction within a small area. The two approaches indicate that the true SMB is about 8 ± 4 % higher than the uncorrected stake-derived estimate. At Dome Fuji, SMB estimates increased by 27 % compared with approaches relying on near-surface density only (Takahashi and Kameda, 2007). At Summit Camp, Greenland, compaction-related underestimation averages 15.12 cm a^{-1} (Howat, 2022).

To quantitatively describe the role of snow densification, researchers have established a series of firn densification models based on empirical and physical principles (Herron & Langway, 1980; Arthern et al., 2010; Li & Zwally, 2015). However, these models have rarely been applied to long-term SMB observation. In this study we use a densification model to simulate the compaction process of snow layers, correcting height changes unrelated to mass change, and thus obtain a relatively accurate estimate of SMB. In addition, high frequency continuous measurements from automatic weather stations (AWS) are

https://doi.org/10.5194/egusphere-2026-2150
Preprint. Discussion started: 27 May 2026

used to estimate surface sublimation and hoar deposition. Sublimation and deposition are important components of surface mass exchange at Dome A (Lenaerts et al., 2019; Ma et al., 2020, 2024). In Dronning Maud Land, surface sublimation can remove 3–9 % of annual solid precipitation, and combined ablation processes during the summer season can remove 15–56 % of solid precipitation (Van den Broeke et al., 2004). At Dome A, where surface melting is absent, sublimation represents the second largest component of the SMB after precipitation. Based on Dome A AWS data from 2005 to 2013, there was a sublimation loss of 2.22 ± 0.02 mm w.e. yr^{-1} and a deposition gain of 1.37 ± 0.02 mm w.e. yr^{-1} (Ding et al., 2016). Under Dome A winter conditions, vapor flux occurs from atmosphere to the snow surface, indicating that hoar deposition dominates over sublimation (Ma et al., 2024). Accurately constraining this flux is critical not only for the regional mass budget but also for interpreting near-surface stratigraphy and for dating ice-core climate records.

The integration of model with in-situ observation provides a framework for refining SMB estimates in the Antarctic interior. In this study, we utilized a firn densification model, driven by ERA5 reanalysis, to simulate firn compaction progress and correct the long-term records at Dome A. Additionally, we quantified the contributions of sublimation and deposition to the SMB using AWS observation, and evaluated the performance of RACMO2.4p1 against the corrected in-situ measurements. This provides a precise SMB benchmark for Dome A and advances the understanding of surface mass exchange processes.

2 Data and method

2.1 Observations

To correct stake-derived SMB for densification and to quantify surface sublimation/deposition — the two key objectives of this study — we utilized two independents in situ datasets: (1) long-term stake array measurements of surface height and density, and (2) high-frequency meteorological observations from an automatic weather station.

2.1.1 Stake array

In 2008, 49 bamboo stakes were installed over 30 × 30 km area around Dome A with a spacing of 5 km (Ding et al., 2015, 2016). Surface height was recorded in 2008, 2011, 2013, 2024, providing three accumulation intervals (2008-2011, 2011-2013, 2013-2024). Near surface snow density was measured at the depth of 0.2 m at each site and was used to convert height change to water-equivalent SMB. Stakes with missing height records in specific period were excluded from the corresponding period mean.

2.1.2 AWS

To analyze the surface energy exchange and quantify sublimation/deposition processes at Dome A, this study uses air temperature, subsurface temperature, wind speed and direction, relative humidity, and surface air pressure data from the Dome A AWS (-80.37° S, 77.37° E). This AWS, built in collaboration with Australia and deployed in 2005, is at an elevation of

https://doi.org/10.5194/egusphere-2026-2150
Preprint. Discussion started: 27 May 2026

4093 m asl and is one of the highest AWS in Antarctica. The dataset is part of the PANDA AWS network which provides important basic information for investigating the energy and mass balance of the Antarctic Plateau (Ding et al., 2022). Prior to use, the AWS data underwent quality control and gap filling.

2.2 ERA5 reanalysis

The fifth generation ECMWF atmospheric reanalysis of global climate was used as the driving data for the firn densification model (Hersbach et al., 2023). ERA5 provides global meteorological fields with a spatial resolution of 0.25° × 0.25°. Monthly surface temperature (Ts) and total precipitation (TP) were obtained for the period 1979 to 2024. We focused on the site at -80.4° S, 77.3° E which is closest to the Dome A AWS. ERA5 captures surface temperature variability reasonably well, and despite uncertainties in precipitation, it provides a continuous dataset suitable for driving firn densification simulation (Roussel et al., 2020; Zhu et al., 2021; Kurita et al., 2025).

2.3 Regional climate model RACMO2.4p1

To provide a spatially and temporally continuous reference for comparison with stake-derived SMB, we used the SMB product from the Regional Atmospheric Climate Model (RACMO) version 2.4p1, developed and maintained by the Royal Netherlands Meteorological Institute (KNMI). RACMO2.4p1 provides gridded SMB at 11 km resolution for 1960–2023 and is widely used for Antarctic SMB assessment (Van Dalum et al., 2024, 2025). Therefore, the densification-corrected stake SMB in this study provides an independent benchmark to evaluate RACMO2.4p1 performance and potential biases over Dome A.

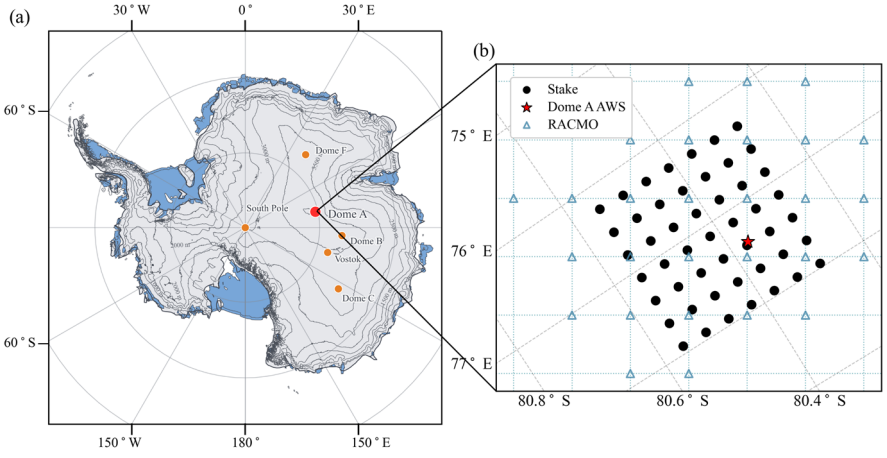

Figure 1: Location of Dome A and the spatial configuration of observations and model grids. **(a)** Map of the AIS showing the location of Dome A (red), Dome B, Dome C, Dome Fuji, Vostok, and South Pole (orange). The black box indicates the region enlarged in panel (b). **(b)** Enlarged view of the Dome A area, showing the distribution of the stake array (black circles), the Dome A AWS (red star), and RACMO grids (blue triangles). The RACMO grids fully cover the spatial extent of the stake array.

https://doi.org/10.5194/egusphere-2026-2150
Preprint. Discussion started: 27 May 2026

2.4 Firn densification model

To quantify surface height changes driven by densification, we apply the Li and Zwally firn densification model developed in 2015 (LZ-2015) to simulate the temporal evolution of the snow column (Li & Zwally, 2015).

LZ-2015 is a semi-empirical model developed for polar firn and based on the classic Herron–Langway (HL) framework (Herron & Langway, 1980), with formulations better suited to Antarctic conditions. Using snow surface temperature and surface accumulation as external forcing, the model computes the transient density profile from the surface to pore close-off depth and outputs the compaction needed to estimate the cumulative subsidence attributable to densification. This model has been applied to several Antarctic interior sites to quantify firn response times to accumulation and temperature variation, including sites on the cold and low accumulation Antarctic plateau such as Vostok.

2.4.1 Model description

Stake measurements record the relative snow surface height change which reflect not only the net mass change but also vertical motion associated with firn compaction. SMB is defined as a mass flux and we adopt the equation of Li and Zwally (2015) to partition the observed height change:

$$\frac{\mathrm{d}H(t)}{\mathrm{d}t} = \frac{A(t)}{\rho_{\mathrm{sf}}} - V_{\mathrm{fc}}(t) - \frac{A_{\mathrm{b}}(t)}{\rho_{\mathrm{i}}} - V_{\mathrm{ice}} + \frac{\mathrm{d}B}{\mathrm{d}t}. \quad (1)$$

In Eq.(1), $\mathrm{d}H(t)/\mathrm{d}t$ is the rate of snow height change. $A(t)$ is the net surface mass input including the net of snowfall, sublimation and hoar deposition, ρ_{sf} is the density of the surface snow, and $A(t)/\rho_{\mathrm{sf}}$ represents the associated surface rise rate. We prescribe ρ_{sf} as the mean snow density measured at 0.2 m depth whose value is approximately 300 kg m^{-3} across the Dome A stake array. $V_{\mathrm{fc}}(t)$ denotes the vertical velocity due to firn densification. $A_{\mathrm{b}}(t)/\rho_{\mathrm{i}}$ is the rate of ablation lowering. V_{ice} denotes the vertical velocity of glacier ice at the firn-ice boundary, and $\mathrm{d}B/\mathrm{d}t$ is the vertical bedrock motion (isostatic uplift). For Dome A, we assume $A_{\mathrm{b}}(t)/\rho_{\mathrm{i}}$, V_{ice}, and $\mathrm{d}B/\mathrm{d}t$ are zero because, respectively, there is no surface melt/runoff , ice dynamics is not considered in a 1-D firn column and bedrock vertical motion is small relative to the surface height changes (Whitehouse et al., 2012).

The time integral of V_{fc} yields cumulative subsidence attributable to compaction. Following the mass conservation formulation of Li and Zwally (2002) , the compaction velocity at depth z is determined by the local density $\rho(z)$ and compaction rate $\mathrm{d}\rho(z)/\mathrm{d}t$:

$$V_{\mathrm{fc}}(z,t) = \int_{z_{\mathrm{i}}}^{z} \frac{1}{\rho(z)} \left[\frac{\mathrm{d}\rho(z)}{\mathrm{d}t}\right] \mathrm{d}z \quad (2)$$

z_{i} is set at the lower boundary of the model, such as the firn-ice transition corresponding to close-off density of 830 kg m^{-3}. The key principle of the LZ-2015 model is to describe the variation of density within the firn column. According to the Li and Zwally (2015) formula, the rate of density change can be expressed as:

$$\frac{\mathrm{d}\rho(z,t)}{\mathrm{d}t} = \beta 8.36(273.2 - T)^{-2.061} A_L(z,t)[\rho_{\mathrm{ice}} - \rho(z,t)] \quad (3)$$

https://doi.org/10.5194/egusphere-2026-2150
Preprint. Discussion started: 27 May 2026

where T is the temperature of the snow layer, calculated with the one-dimensional heat conduction equation; ρ_{ice} is the density of pure ice, which is 917 kg m^{-3}; $\rho(z,t)$ is the density at depth z and time t; and $A_L(z,t)$ is the local accumulation rate that governs overburden loading and thus drives compaction.

$$A_{\mathrm{L}}(z,t) = 1/t_{\mathrm{z}} \int_{t_z=0 \text{ to } t_z} A(t_{\mathrm{z}})\mathrm{d}t_{\mathrm{z}} \quad (4)$$

where t_{z} denotes the time for a snow layer initially at the surface to reach depth z through accumulation and compaction. $A_{\mathrm{L}}(z,t)$ represents the average temporal evolution of the overlying load acting on a firn layer at that depth, which propagates in response to changes in surface accumulation.

The empirical parameter β is constrained by matching simulated and observed density profiles. Following LZ-2015, β is defined piecewise for two density regimes:

$$\beta_1 = \beta_{scale1}(-1.218 - 0.403T_{\mathrm{m}}) \ (\rho \le 550) \quad (5)$$

$$\beta_2 = \beta_{scale2}\beta_1(0.792 - 1.080A_{\mathrm{m}} + 0.00465T_{\mathrm{m}}) \ (\rho > 550) \quad (6)$$

where A_{m} is the long-term mean accumulation rate at the site and T_{m} is the mean annual surface temperature. A_{m} and T_{m} are calculated as multi-year means from the forcing dataset. These two stages respectively describe rapid densification in shallow layers, when the density is less than 550 kg m^{-3}, and slow densification in deep layers, when the density is greater than 550 kg m^{-3}. From ice-core measurements at Dome A, the firn reached the close-off density of approximately 830 kg m^{-3} at a depth of 71 m, which provides an observational constraint. To enhance the applicability of the model to low temperature and low accumulation, this study introduces two independent dimensionless coefficients β_{scale1} and β_{scale2} to the LZ-2015 empirical formulation. This approach allows adjustment for the rapid and slow densification process independently without changing their corresponding relationship. We regard them as calibration parameters: β_{scale1} was optimized to match the observed depth of 18.05 m where the density reaches 550 kg m^{-3}, while β_{scale2} was determined based on the close-off depth of 71.08 m where the density reaches 830 kg m^{-3}.

2.4.2 Model configuration and calibration

The firn column was extended to 120 m and discretized into 12000 uniform vertical layers with a layer thickness of 1 cm. The model is advanced with a monthly time step, consistent with the temporal resolution of the ERA5 forcing data. At each time step, monthly surface temperature and total precipitation are prescribed to update the temperature field, overburden loading, density evolution, and vertical displacement of the snow layer.

Model experiments comprise two stages:

1. Spin-up: using ERA5 mean temperature and accumulation over 1979-2010 as climatological forcing, we ran a 2700 years integration to achieve a quasi-equilibrium. The climatological values from this are -51.29 °C and 0.016 m w.e. yr^{-1}. A dual-stage calibration was implemented to determine the optimal scaling factors. β_{scale1} was determined to be 2.10, ensuing the simulated density reached 550 kg m^{-3} at 18.05 m; and β_{scale2} was determined to be 3.86, to give a close-off depth of 71.08 m. The resulting density profiles are analyzed in Sect.3.1.

https://doi.org/10.5194/egusphere-2026-2150
Preprint. Discussion started: 27 May 2026

2. Transient Simulation: the spin-up output was used as the initial condition, and the model was integrated forward under time-varying ERA5 forcing to simulate the temporal evolution of the firn density profile and the associated surface elevation change due to densification.

2.5 Estimation of sublimation

Sublimation at Dome A was calculated using the bulk-aerodynamic method (Oke, 1987). LE is expressed as:

$$\mathrm{LE} = \rho L_s C_E u(q - q_s) \quad (7)$$

where ρ is the density of air (calculated as $\rho = (\rho_0 P)/P_0$); L_s is the latent heat of sublimation (2.834 MJ kg^{-1}); the bulk transfer coefficient C_E is set to 0.00129 under stable atmospheric conditions and to 0.002 under unstable conditions; u is the 4 m wind speed; q and q_s are the specific humidity at 4 m and at the snow surface, calculated using the saturation vapor pressure e_s (Bolton, 1980).

$$q_s \approx \varepsilon e_s / p \ (\varepsilon = 0.622) \quad (8)$$

$$e_s = 6.112 \exp\left[\frac{17.67 T_s}{T_s + 243.5}\right] \quad (9)$$

The sublimation rate M_s was obtained from $M_s = LE/L_s$. When the process is deposition, M_s takes a negative value.

3 Results

3.1 Density profile

Across the full firn column, density increases monotonically with depth, and the simulated 2024 density profile agrees well with the ice-core observation (Fig.2a). The density of the ice core is measured using the gravimetric method. When the core geometry is well preserved, this method can provide a relatively reliable estimate of density, whereas biases are more likely to occur in low density snow (Morris and Cooper, 2003; Hawley et al., 2008). This simulation captures the process by which each snow layer is gradually compacted under the influence of overlying pressure and temperature. The surface density started at 300 kg m^{-3}, in good agreement with the mean measured from the stake array. At depth of 18.05 m, the density reached 550 kg m^{-3}, where the near-surface firn is mainly driven by rearrangement and packing of snow grains. Over the intervening depth, the density profile exhibited a steep slope, indicating that the compaction of the shallow layer of snow occurs rapidly. When the density exceeds 550 kg m^{-3}, pressure sintering became the dominant mechanism, and the densification rate slowed down (Ebinuma and Maeno, 1985; Stevens et al., 2023). Our simulated profile aligns with the structural transition of the firn column, reaching the close-off density of 830 kg m^{-3} at 71.08 m, where air in the firn is almost completely isolated from the atmosphere and most air becomes isolated in bubbles (Jang et al., 2019; Westhoff et al., 2024). The model reproduces the overall shape of density-depth profile well, indicating that the inclusion of these two constraint points is necessary.

To focus on the compaction process directly relevant to stake measurements, we examined the near-surface firn variation in detail by magnifying the density profile for the upper 0-5 m (Fig.2b). Specifically, the selected times of profile correspond to

https://doi.org/10.5194/egusphere-2026-2150
Preprint. Discussion started: 27 May 2026

the period of the stake observation. The 2024 density profile shows a rapid increase from 300 kg m^{-3} at the surface to about 385 kg m^{-3} at 5 m depth. Such a sharp change in density reflects pronounced surface compaction, which is a key source of bias in SMB derived from the stake measurements. The black dotted line in Fig.2b indicates that the 2008 surface was located 0.87 m below the 2024 surface. This depth represents the position of 2008 surface after 16 years of accumulation and compaction. The 2024 density values are higher than 2008 by approximately 13-17 kg m^{-3} at all equivalent depths, as quantified by the $\Delta\rho$ profile (purple), suggesting that the shallow snow experienced significant densification over this time. Continuous snowfall at the surface gradually pushes the underlying layers downward and compacts them year by year. If the process of compaction is ignored, the densification-driven subsidence embedded in the stake-recorded surface height change is not accounted for, leading to an underestimation of the SMB. In this study, we isolated and removed the height change associated with densification to obtain a corrected, more accurate SMB.

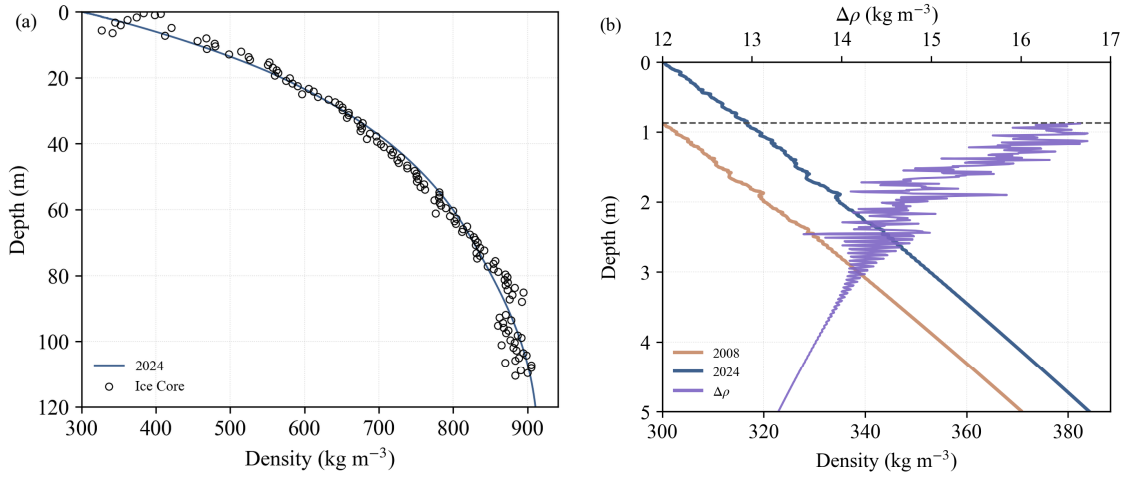

Figure 2: (a) Simulated density profile for 2024 (blue line) compared with the observed ice-core density (open circles). **(b)** Comparison of the simulated density profiles for 2008 (orange) and 2024 (blue) in the upper 5 m. $\Delta\rho$ (purple line) indicates the density difference between 2024 and 2008 at equivalent depths. The dashed line marks the position of the 2008 surface, which is buried to about 0.87 m below the 2024 surface.

3.2 Long-term cumulative subsidence

From the derived high resolution density profiles, we quantified the subsidence of the entire snow layer due to compaction. Figure 3a shows the time series of cumulative subsidence of the entire firn column from 1979-2024. The cumulative subsidence increases linearly, suggesting a stable climate at Dome A, and accordingly, the overall compaction rate is also relatively stable. The total subsidence over the entire period reached 2.68 m. To match the period of stake observation, this study calculated the cumulative subsidence of the entire firn column from 2008 to 2024. Over these 16 years, the subsidence caused by compaction is 0.959 m. This magnitude of subsidence underscores the necessity of correcting stake measurements for densification. Figure

https://doi.org/10.5194/egusphere-2026-2150
Preprint. Discussion started: 27 May 2026

3b illustrates the influence of firn densification on snow layer and stake measurements. As the snow compacts, the 2008 surface is buried beneath the 2024 surface, while the stake descends with the surrounding snow layers. Consequently, this cumulative subsidence cannot be used for stake correction.

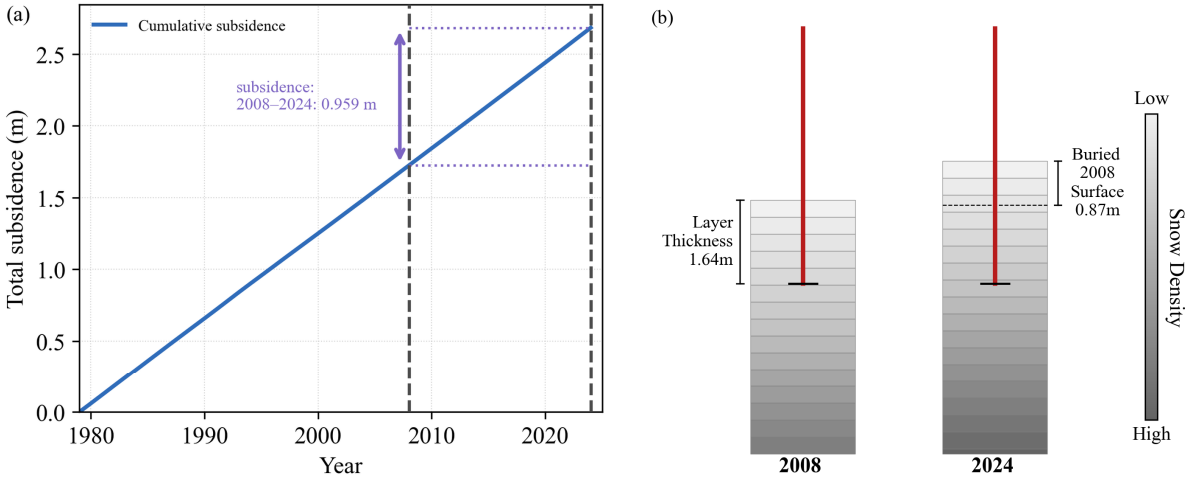

Figure 3 (a) Simulated cumulative subsidence caused by firn densification from 1980 to 2024. The dashed vertical lines mark 2008 and 2024, and the purple arrow indicates a subsidence of 0.959 m between the two years. **(b)** Schematic illustration of the relative positions of the 2008 and 2024 surfaces with the stake bottoms aligned to the same level. The dashed horizontal line marks the buried 2008 surface, located 0.87 m below the 2024 surface, and the grey shading indicates increasing snow density with depth.

3.3 Simulation of subsidence at the stake-bottom depth

The stake measurement records the distance from the top of the stake to the snow surface. Because the stakes descend with the surrounding firn layers, the densification occurring below the stakes base does not influence the readings. We only need to consider the compaction between the snow surface and the stake base. This process caused the snow surface to descend relative to the stake, thereby reducing the measured height increase and resulting in SMB being underestimated. It is important to emphasize that the surface lowering only refers to the effect of firn densification. In reality, when deposition and snowfall are included, the total snow surface relative to the stake may rise. In this study, the average insertion depth of the stakes is approximately 1.64 m. The LZ-2015 model was used to simulate the total subsidence at this depth from 2008 to 2024 (Fig.4). Since in practice the stakes were inserted to slightly different depths, this study designed two sensitivity simulations. The initial depths were set to 0.8 m and 3 m respectively, and simulated the total subsidence of both depths from 2008 to 2024. Figure 4 shows the time series of cumulative subsidence for the three depths. For the mean insertion depth of 1.64 m, the cumulative subsidence reached 0.104 m over the 16-year period. For the stake inserted relatively shallowly (0.8 m), the cumulative subsidence reached 0.067 m. For the deeper stake (3 m), due to the thicker overlying firn column, the cumulative subsidence is larger reaching 0.160 m. By incorporating the subsidence value into the readings of the surface height change, we obtained a corrected and more reliable SMB estimate. The mean annual SMB is 22.19 kg $m^{-2}yr^{-1}$ without correction from 2008 to 2024. When corrected for densification at a stake base depth of 1.64 m, the value increases to 24.14 kg $m^{-2}yr^{-1}$. The firn

https://doi.org/10.5194/egusphere-2026-2150
Preprint. Discussion started: 27 May 2026

densification bias constitutes about 8.8 % of the uncorrected SMB estimates. These results clearly indicate that in low temperature and low accumulation environments such as Dome A, firn densification substantially influence the accuracy of stake measurement of SMB. Therefore, the correction method proposed in this study is essential for obtaining precise SMB estimates in Dome A.

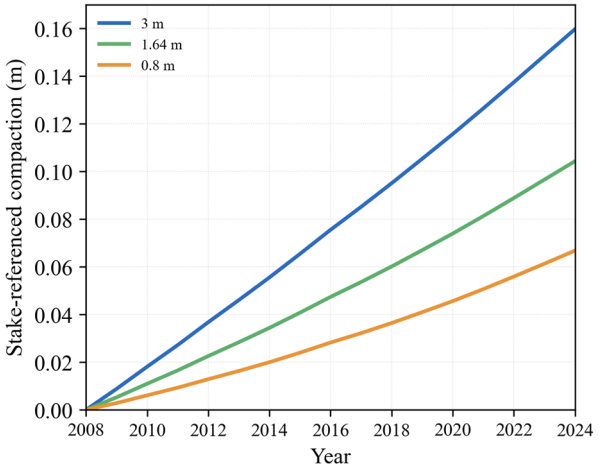

Figure 4 Cumulative subsidence simulated by the LZ-2015 model for 2008-2024 for stakes inserted to different base depths (0.8 m, 1.64 m, 3 m). The simulation results are shown for the mean stake depth of 1.64 m, as well as for 0.8 m and 3.0 m depths, which are used to estimate the lower and upper bounds of uncertainty.

3.4 Spatial distribution of SMB

3.4.1 Spatial distribution of observed SMB

The spatial distribution of SMB over Dome A during 2008-2024 was obtained from stake observation. The entire observation period was divided into 2008-2013 and 2013-2024, and the overall mean SMB for 2008-2024 was also presented after correction using the firn densification model (Fig.5). During 2008-2013, SMB exhibited strong spatial variability, with alternating local maxima and minima with values ranging from 14.8 to 40.7 kg $m^{-2}yr^{-1}$ (Fig.5a). In the period 2013-2024, the SMB distribution experienced changes: the peak of high SMB region declined, and one of the previous high SMB zones at -80.45° S, 76.6° E became a low zone (Fig.5b). The two periods exhibit different SMB spatial patterns, indicating that the distribution is not temporally stationary. Over the entire period from 2008 to 2024, the long-term SMB distribution was smoother (Fig.5c). The spatial distribution of SMB displays a clear trend, characterized by high value in the northwest and low value elsewhere, with the high region averaging above 29 kg $m^{-2}yr^{-1}$. At Dome A, observations show no prevailing wind direction. The observed SMB heterogeneity is more plausibly linked to wind-driven snow redistribution controlled by local topography. Higher wind speeds over local topographic highs can enhance snow erosion, whereas reduced wind speeds in adjacent lower-elevation areas can favour snow redeposition, which may contribute to the formation of local high-SMB zones.

https://doi.org/10.5194/egusphere-2026-2150
Preprint. Discussion started: 27 May 2026

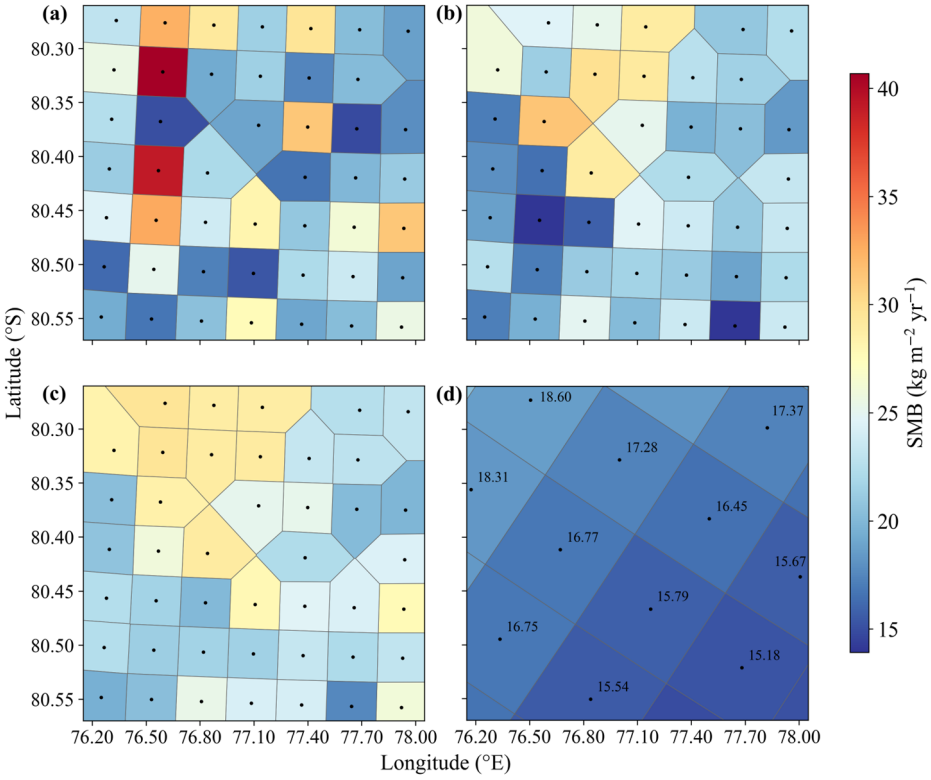

Figure 5 (a) Mean annual SMB from 2008 to 2013 derived from stake observations. **(b)** Mean annual SMB from 2013 to 2024 derived from stake observations. **(c)** Mean annual SMB from 2008 to 2024 after densification correction. **(d)** Mean annual SMB from 2008 to 2024 simulated by the RACMO2.4p1 model. Black dots indicate stake locations in (a)–(c) and RACMO grids in (d). Some stakes are missing in certain years, so the number of available stake observations vary slightly among the panels.

3.4.2 Spatial distribution of SMB from RACMO

To evaluate the capability of the regional climate model to simulate the spatial distribution of SMB over Dome A, this study used the RACMO2.4p1 at a horizontal resolution of 11 km from 2008 to 2024 (Van Dalum et al., 2025). The results show that RACMO exhibits a gradient decreasing from northwest to southeast gradient, indicating that the model response to topographic forcing is relatively accurate (Fig.5d). However, the SMB simulated by RACMO exhibits greater spatial homogeneity compared to observations, with a notably reduced amplitude of variability. This discrepancy arises because RACMO provides grid-cell mean SMB at 11 km resolution, which suppresses sub-grid spatial variability, whereas stake observations capture highly localized SMB variations driven by wind redistribution interacting with surface micro-relief (sastrugi and dunes), thereby producing larger point-scale contrasts (Richter et al., 2021; Cavitte et al., 2023; Stefanini et al., 2025). The mean annual SMB of RACMO for this period is 17.50 kg $m^{-2}yr^{-1}$, which is considerably lower than the corrected observational value of 24.14 kg $m^{-2}yr^{-1}$. Such underestimation has also been reported in the 2 km resolution RACMO simulation (Noël et al., 2023). Although RACMO performed well in simulating the large-scale SMB trend of the Antarctic ice sheet, the simulation of local SMB in the low accumulation, wind-affected Dome A region remains limited by the current resolution and

https://doi.org/10.5194/egusphere-2026-2150
Preprint. Discussion started: 27 May 2026

parameterization schemes. High-resolution SMB observations with densification correction as obtained in this study can provide crucial data for the improvement of regional climate models.

3.5 Sublimation and deposition at Dome A

Using the bulk-aerodynamic formulation described in Sect.2.5, sublimation rates for 2005 to 2024 were derived from the Dome A AWS data. To reduce the impact of discontinuities in the winter wind speed observations, this study used the daily-mean wind speed instead of instantaneous hourly values. When an entire day was missing, the climatological mean was used to fill the gaps. Based on the 19-year averages of daily means, the total sublimation is 2.34 mm w.e. yr^{-1}, occurring mostly between November and January in summer, while the total deposition is 0.87 mm w.e. yr^{-1}, primarily between February and April (Fig.6). Overall, the gross annual surface mass input at Dome A is estimated to be 25.61 kg $m^{-2}yr^{-1}$. Net surface vapor flux removes 1.47 mm w.e. yr^{-1}, leaving a densification-corrected net SMB of 24.14 kg $m^{-2}yr^{-1}$. Thus, the net deposition-sublimation equivalent to 5.7 % of the total input or 6.1 % of the estimated mean net SMB. Despite sublimation constituting a relatively small fraction of the net SMB, it plays a role in the long-term evolution of surface snow structure. Sublimation leads to preferential loss of lighter isotopes, altering the isotopic composition and ion concentration characteristics of ice core (Hoshina et al., 2014; Ma et al., 2024). Although the long-term mean LE is less than 3 W m^{-2}, it remains an important turbulent heat loss component of the surface energy balance. Therefore, quantitative characterization of sublimation and deposition is essential for accurately assessing the energy-mass balance and is crucial for interpreting snow composition changes and high-resolution ice core records.

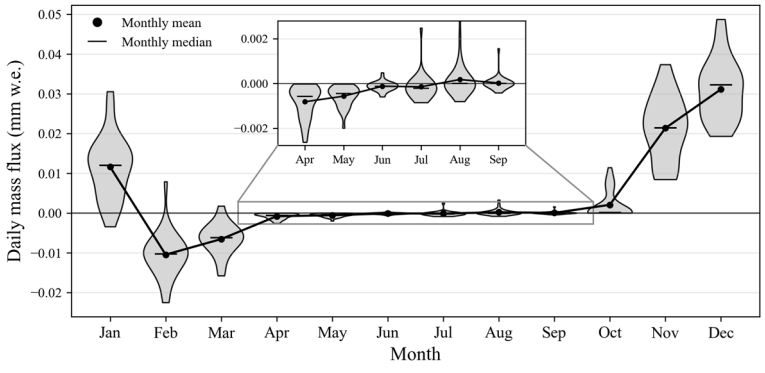

Figure 6 Monthly distribution of daily mass flux derived from Dome A AWS observations from 2005-2024. Positive values indicate sublimation and negative values indicate deposition. Violin plots show the distribution of daily mean values for each month, with width representing probability density. Black circles denote the monthly mean, and short horizontal bars denote the monthly median. The inset shows an enlarged view for April to September.

https://doi.org/10.5194/egusphere-2026-2150
Preprint. Discussion started: 27 May 2026

4 Discussion

4.1 Correction for stake observation

While firn compaction is often negligible in high accumulation regions over short observation periods, our results demonstrate that it becomes a critical source of bias in the low-accumulation environment of Dome A. The cumulative subsidence over decadal timescales constitutes a considerable fraction of the observed surface height change and cannot be ignored. Based on the LZ-2015 firn densification model forced by ERA5 reanalysis, this study simulated the densification of a 120 m firn column from 1979 to 2024 and at the average depth of stake base (1.64 m) from 2008 to 2024. The results show that the surface subsidence can reach the order of ten centimetres over the 16 years. Consequently, neglecting the effect of densification will lead to an underestimation of the actual SMB. By compensating for densification-driven surface lowering in stake measurements, we removed height variations unrelated to mass change, yielding a more accurate SMB estimate.

Previous studies have proposed several approaches to correct systematic biases in stake-derived SMB, though the magnitude of correction is not always directly comparable. For instance, at Dome Fuji, the large correction of about 27 % mainly reflects a density correction rather than an exceptionally strong compaction correction. Kameda used the average snow density at the stake base to convert height change to water-equivalent, implicitly accounting for compaction effects via the selection of a representative density (Kameda et al., 2008; Takahashi and Kameda, 2007). In contrast, Vostok and Dome A (this study) directly correct the densification-induced lowering of the snow firn column between the stake base and surface. Ekaykin et al. (2020) recommended a smaller empirical correction of 8 ± 4 % on total SMB at Vostok. At Dome C, Stefanini et al. (2025) corrected stake-derived SMB with the formulation of Ekaykin, increasing the mean SMB from 26.29 to 27.21 kg $m^{-2}yr^{-1}$, corresponding to a correction of 3.5 %. The much larger correction reported at Dome Fuji, relative to the smaller corrections at Vostok, Dome C, and Dome A, arises mainly from differences in correction strategy rather than an enhance firn densification rate at Dome Fuji itself.

4.2 Sources of uncertainty in correction

Recent studies have shown that uncertainties in firn compaction are mainly controlled by the choice of climate forcing, the formulation of densification, and empirical parameters (Verjans et al., 2021; Veldhuijsen et al., 2023). This study at Dome A is subject to similar sources of uncertainty, primarily stemming from the climate forcing data and the semi-empirical nature of the model. The model is forced with surface temperature and total precipitation from the ERA5 reanalysis. However, in the interior of Antarctica, where observational data is extremely scarce, the accuracy of ERA5 is limited. Previous evaluations indicate that ERA5 exhibits a warm bias at inland sites and a dry bias over the east Antarctic plateau (Zhu et al., 2021; Wang et al., 2021). Combining these assessments with the climatological constraints reported by Xiao et al. (2008b) and Hou et al. (2007), setting the long-term mean temperature and accumulation to -58.3 °C and 0.023 m w.e. yr^{-1} could lead to an estimated ~ 0.8 % change in the densification-corrected SMB. These biases inevitably propagate into the simulated density profiles and compaction rates. The LZ-2015 model is a semi-empirical model originally calibrated for

https://doi.org/10.5194/egusphere-2026-2150
Preprint. Discussion started: 27 May 2026

typical Antarctic conditions. Modest changes in empirical parameters can lead to compaction rate differences of tens of percent (Horlings et al., 2021; Stevens et al., 2023). To reduce parameter uncertainty for Dome A, we used two independent scaling factors. Nevertheless, residual uncertainty remains because the calibration relies on limited observational constraints. Without applying the scaling factor, the subsidence of 1.64 m snow layer is limited to 0.05 m, leading to an SMB change that is approximately 50 % of that obtained with scaling. In the estimation of sublimation and deposition, uncertainties may arise from the precision of AWS instruments and from the reconstruction method of wind speed, leading to uncertainties in the estimated contribution of sublimation and deposition to the SMB. At Panda-1 (74°39′S, 77°E; 2,737 m asl), Ding et al. (2020) quantified that a ±5 % perturbation in relative humidity can alter the latent heat flux by +22.7 %/−31.8 %, while a −1.5 m s^{-1} wind-speed bias leads to a −26 % change in latent heat flux. A similar sensitivity is reported for Dome A: Yang et al. (2025) showed that increasing the wind speed by +1.5 m s^{-1} could induce an approximately −28.5 % change in LE. These results indicate that uncertainty in wind, moisture and reconstruction methods can translate to uncertainty in the sublimation contribution to SMB. This is particularly relevant for the Antarctic interior, where the absolute magnitude of LE is small and thus its relative sensitivity to input perturbations is high.

4.3 Climatic significance of accurate SMB evaluation in Dome Argus

Despite existing uncertainties, accurately assessing the surface mass balance (SMB) of AIS holds important climatic significance. Antarctica lost 2671 ± 530 Gt over 1992-2020, contributing 7.4 ± 1.5 mm to global mean sea-level rise (Otosaka et al., 2023). Moreover, the Antarctic-integrated SMB is of order ~ 2.3-2.5 × 10^3 Gt yr^{-1}, but estimates from different models still differ by several hundred Gt yr^{-1}, underscoring the importance of independent observational benchmarks (Mottram et al., 2021; Van Dalum et al., 2025). Meanwhile, firn processes are a leading limitation for altimetry-based mass-balance estimates, with uncertainties in firn thickness changes reaching ~ 20-108 % at the basin-mean scale and ~ 54-186 % at the grid-cell scale (Lundin et al., 2017; Kappelsberger et al., 2024). In addition, vapor exchange over the Antarctic interior cannot be climatically negligible. At Dome C, net annual sublimation of 3.1-3.7 mm w.e. yr^{-1} accounts for ~ 12-15 % of the annual SMB, while post-depositional processes markedly alter the primary precipitation signal recorded in firn (Ollivier et al., 2025). The sublimation and deposition processes play an important role in SMB, helping to interpret the depositional noise in ice core archives and offering guidance for future ice core drilling in the Dome A.

5 Conclusion

Based on the stake array observation from 2008 to 2024 in the Dome A, Antarctica, this study quantitatively corrected the error of SMB caused by snow surface subsidence due to firn densification using the LZ-2015 model driven by ERA5 reanalysis data. Furthermore, AWS observations were used to analyze the sublimation and deposition processes in this region.

We found that firn densification is a major source of error in stake method estimation of SMB. Over the 16-year period, the cumulative subsidence at the mean stake-base depth of 1.64 m reached 0.104 m. The uncorrected SMB (22.19 kg $m^{-2}yr^{-1}$)

https://doi.org/10.5194/egusphere-2026-2150
Preprint. Discussion started: 27 May 2026

was increased by approximately 8.8 % after correction, giving a more accurate SMB estimate of 24.14 kg $m^{-2}yr^{-1}$.

We also found that the short-term SMB in the Dome A region is affected by local topography and winds and has spatial variability, especially in the northwestern sector. However, this spatial variability is not captured by RACMO2.4p1. In addition, the corrected SMB (24.14 kg $m^{-2}yr^{-1}$) is higher than the RACMO simulation (17.50 kg $m^{-2}yr^{-1}$), suggesting that the current version of the regional climate model may underestimate mass input over the Antarctic interior.

We estimated the total sublimation at Dome A as 2.34 mm w.e. yr^{-1}, while deposition is 0.87 mm w.e. yr^{-1}, resulting in a net loss of 1.47 mm w.e. yr^{-1}. The net deposition-sublimation accounts for approximately 5.7 % of the total input, or 6.1 % of the estimated mean net SMB. Although the absolute values are small, their contribution to SMB is high, exerting a notable impact on SMB.

The method proposed in this study, which integrates stake observation with a firn densification model, offers an effective way to obtain accurate SMB in cold and low accumulation environments. This methodology applies to other inland ice sheets in Antarctica, such as Dome Fuji and Vostok, as well as high-altitude regions of Greenland and glaciers in Tibet. We recommend carrying out more ice core density profile measurements onsite. The high-quality data would be valuable to optimize the empirical parameters, thereby further improving SMB calculations based on the regional climate models.

Code and data availability

The stake observations data is prepared for public release through the Chinese National Arctic and Antarctica Data Center. The dataset DOI will be added to this section once it becomes available. Before the public release is completed, the stake observations data and model code are available upon request to Minghu Ding (email: dingminghu@foxmail.com). ERA5 reanalysis data are available at https://doi.org/10.24381/cds.f17050d7 (Hersbach et al., 2023). Monthly RACMO2.4p1 data for the SMB are available at https://doi.org/10.5281/zenodo.19255213 (Van Dalum et al., 2026). The Dome A AWS data is publicly available from https://doi.org/10.26179/brjy-g225 (Heil et al., 2017).

Author contributions

The study was designed by XZ and MD. The firn densification simulations were carried out by XZ. MD supervised the study. DY contributed to the analysis of surface vapor flux. KZ, IA and PH provide support for Antarctic data. BC, IA, YY, XC, CL and CX contributed to manuscript review and improvement.

Competing interests

At least one of the (co-)authors is a member of the editorial board of *The Cryosphere*. The authors have no other competing interests to declare.

https://doi.org/10.5194/egusphere-2026-2150
Preprint. Discussion started: 27 May 2026

Acknowledgements

The stake observations were carried out during the Chinese National Antarctic Research Expedition (CHINARE) from Zhongshan Station to Dome A. We gratefully acknowledge the members for their efforts in establishing, maintaining, and remeasuring the stake array.

Financial support

This work was supported by National Natural Science Foundation of China (42525607), Basic Research Fund of CAMS (2023Z015, 2023Z004 and 2023Z025).

References

Arthern, R. J., Vaughan, D. G., Rankin, A. M., Mulvaney, R., and Thomas, E. R.: In situ measurements of Antarctic snow compaction compared with predictions of models, Journal of Geophysical Research: Earth Surface, 115, F03011, https://doi.org/10.1029/2009JF001306, 2010.

Bolton, D.: The computation of equivalent potential temperature., Monthly Weather Review, 108, 1046–1053, https://doi.org/10.1175/1520-0493(1980)108%3C1046:TCOEPT%3E2.0.CO;2, 1980.

Cavitte, M. G. P., Goosse, H., Matsuoka, K., Wauthy, S., Goel, V., Dey, R., Pratap, B., Van Liefferinge, B., Meloth, T., and Tison, J.-L.: Investigating the spatial representativeness of East Antarctic ice cores: a comparison of ice core and radar-derived surface mass balance over coastal ice rises and Dome Fuji, The Cryosphere, 17, 4779–4795, https://doi.org/10.5194/tc-17-4779-2023, 2023.

Cui, X., Sun, B., Tian, G., Tang, X., Zhang, X., Jiang, Y., Guo, J., and Li, X.: Ice radar investigation at Dome A, East Antarctica: Ice thickness and subglacial topography, Chin. Sci. Bull., 55, 425–431, https://doi.org/10.1007/s11434-009-0546-z, 2010.

Diener, T., Sasgen, I., Agosta, C., Fürst, J. J., Braun, M. H., Konrad, H., and Fettweis, X.: Acceleration of dynamic ice loss in Antarctica from satellite gravimetry, Front. Earth Sci., 9, https://doi.org/10.3389/feart.2021.741789, 2021.

Ding, M., Xiao, C., Li, C., Qin, D., Jin, B., Shi, G., Xie, A., and Cui, X.: Surface mass balance and its climate significance from the coast to Dome A, East Antarctica, Sci. China Earth Sci., 58, 1787–1797, https://doi.org/10.1007/s11430-015-5083-9, 2015.

Ding, M., Xiao, C., Yang, Y., Wang, Y., Li, C., Yuan, N., Shi, G., Sun, W., and Ming, J.: Re-assessment of recent (2008–2013) surface mass balance over Dome Argus, Antarctica, Polar Research, 35, 26133, https://doi.org/10.3402/polar.v35.26133, 2016.

Ding, M., Yang, D., Van den Broeke, M. R., Allison, I., Xiao, C., Qin, D., and Huai, B.: The surface energy balance at Panda 1 Station, Princess Elizabeth Land: A typical katabatic wind region in East Antarctica, Journal of Geophysical Research: Atmospheres, 125, e2019JD030378, https://doi.org/10.1029/2019JD030378, 2020.

https://doi.org/10.5194/egusphere-2026-2150
Preprint. Discussion started: 27 May 2026

Ding, M., Zou, X., Sun, Q., Yang, D., Zhang, W., Bian, L., Lu, C., Allison, I., Heil, P., and Xiao, C.: The PANDA automatic weather station network between the coast and Dome A, East Antarctica, Earth System Science Data, 14, 5019–5035, https://doi.org/10.5194/essd-14-5019-2022, 2022.

Ebinuma, T. and Maeno, N.: Experimental studies on densification and pressure-sintering of ice, Annals of Glaciology, 6, 83–86, https://doi.org/10.3189/1985AoG6-1-83-86, 1985.

Eisen, O., Frezzotti, M., Genthon, C., Isaksson, E., Magand, O., Van den Broeke, M. R., Dixon, D. A., Ekaykin, A., Holmlund, P., Kameda, T., Karlöf, L., Kaspari, S., Lipenkov, V. Y., Oerter, H., Takahashi, S., and Vaughan, D. G.: Ground-based measurements of spatial and temporal variability of snow accumulation in East Antarctica, Reviews of Geophysics, 46, RG2001, https://doi.org/10.1029/2006RG000218, 2008.

Ekaykin, A. A., Teben'kova, N. A., Lipenkov, V. Ya., Tchikhatchev, K. B., Veres, A. N., and Richter, A.: Underestimation of snow accumulation rate in Central Antarctica (Vostok Station) derived from stake measurements, Russ. Meteorol. Hydrol., 45, 132–140, https://doi.org/10.3103/S1068373920020090, 2020.

Hawley, R. L., Brandt, O., Morris, E. M., Kohler, J., Shepherd, A. P., and Wingham, D. J.: Techniques for measuring high-resolution firn density profiles: case study from Kongsvegen, Svalbard, Journal of Glaciology, 54, 463–468, https://doi.org/10.3189/002214308785837020, 2008.

Heil, P., Hyland, G., and Alison, I.: Automatic Weather Station Data obtained at Dome A (Argus), Antarctica, Ver. 1, Australian Antarctic Data Centre [data set], https://doi.org/10.26179/brjy-g225, 2017.

Herron, M. M. and Langway, C. C., Jr.: Firn densification: An empirical model, Journal of Glaciology, 25, 373–385, https://doi.org/10.3189/S0022143000015239, 1980.

Hersbach, H., Bell, B., Berrisford, P., Biavati, G., Horányi, A., Muñoz Sabater, J., Nicolas, J., Peubey, C., Radu, R., Rozum, I., Schepers, D., Simmons, A., Soci, C., Dee, D., and Thépaut, J.-N.: ERA5 monthly averaged data on single levels from 1940 to present, Copernicus Climate Change Service (C3S) Climate Data Store (CDS), [data set], https://doi.org/10.24381/CDS.F17050D7, 2023.

Horlings, A. N., Christianson, K., Holschuh, N., Stevens, C. M., and Waddington, E. D.: Effect of horizontal divergence on estimates of firn-air content, Journal of Glaciology, 67, 287–296, https://doi.org/10.1017/jog.2020.105, 2021.

Hoshina, Y., Fujita, K., Nakazawa, F., Iizuka, Y., Miyake, T., Hirabayashi, M., Kuramoto, T., Fujita, S., and Motoyama, H.: Effect of accumulation rate on water stable isotopes of near-surface snow in inland Antarctica, JGR Atmospheres, 119, 274–283, https://doi.org/10.1002/2013JD020771, 2014.

Hou, S., Li, Y., Xiao, C., and Ren, J.: Recent accumulation rate at Dome A, Antarctica, CHINESE SCI BULL, 52, 428–431, https://doi.org/10.1007/s11434-007-0041-3, 2007.

Howat, I. M.: Temporal variability in snow accumulation and density at Summit Camp, Greenland Ice Sheet, Journal of Glaciology, 68, 1076–1084, https://doi.org/10.1017/jog.2022.21, 2022.

Jang, Y., Hong, S. B., Buizert, C., Lee, H.-G., Han, S.-Y., Yang, J.-W., Iizuka, Y., Hori, A., Han, Y., Jun, S. J., Tans, P., Choi, T., Kim, S.-J., Hur, S. D., and Ahn, J.: Very old firn air linked to strong density layering at Styx Glacier, coastal Victoria Land, East Antarctica, The Cryosphere, 13, 2407–2419, https://doi.org/10.5194/tc-13-2407-2019, 2019.

https://doi.org/10.5194/egusphere-2026-2150
Preprint. Discussion started: 27 May 2026

Kameda, T., Motoyama, H., Fujita, S., and Takahashi, S.: Temporal and spatial variability of surface mass balance at Dome Fuji, East Antarctica, by the stake method from 1995 to 2006, Journal of Glaciology, 54, 107–116, https://doi.org/10.3189/002214308784409062, 2008.

Kappelsberger, M. T., Horwath, M., Buchta, E., Willen, M. O., Schröder, L., Veldhuijsen, S. B. M., Kuipers Munneke, P., and van den Broeke, M. R.: How well can satellite altimetry and firn models resolve Antarctic firn thickness variations?, The Cryosphere, 18, 4355–4378, https://doi.org/10.5194/tc-18-4355-2024, 2024.

Kurita, N., Bromwich, D. H., Kameda, T., Motoyama, H., Hirasawa, N., Mikolajczyk, D. E., Keller, L. M., and Lazzara, M. A.: Summer warming in the East Antarctic interior triggered by southern Indian Ocean warming, Nat Commun, 16, 6764, https://doi.org/10.1038/s41467-025-61919-3, 2025.

Lenaerts, J. T. M., Medley, B., Van den Broeke, M. R., and Wouters, B.: Observing and modeling ice sheet surface mass balance, Rev Geophys, 57, 376–420, https://doi.org/10.1029/2018RG000622, 2019.

Li, J. and Zwally, H. J.: Modeled seasonal variations of firn density induced by steady-state surface air-temperature cycle, Annals of Glaciology, 34, 299–302, https://doi.org/10.3189/172756402781817707, 2002.

Li, J. and Zwally, H. J.: Modeling of firn compaction for estimating ice-sheet mass change from observed ice-sheet elevation change, Annals of Glaciology, 52, 1–7, https://doi.org/10.3189/172756411799096321, 2011.

Li, J. and Zwally, H. J.: Response times of ice-sheet surface heights to changes in the rate of Antarctic firn compaction caused by accumulation and temperature variations, Journal of Glaciology, 61, 1037–1047, https://doi.org/10.3189/2015JoG14J182, 2015.

Lundin, J. M. D., Stevens, C. M., Arthern, R., Buizert, C., Orsi, A., Ligtenberg, S. R. M., Simonsen, S. B., Cummings, E., Essery, R., Leahy, W., Harris, P., Helsen, M. M., and Waddington, E. D.: Firn Model Intercomparison Experiment (FirnMICE), Journal of Glaciology, 63, 401–422, https://doi.org/10.1017/jog.2016.114, 2017.

Ma, T., Li, L., Shi, G., and Li, Y.: Acquisition of post-depositional effects on stable isotopes (δ18O and δD) of snow and firn at Dome A, East Antarctica, Water, 12, 1707, https://doi.org/10.3390/w12061707, 2020.

Ma, T., Jiang, Z., Ding, M., He, P., Li, Y., Zhang, W., and Geng, L.: A model framework for atmosphere–snow water vapor exchange and the associated isotope effects at Dome Argus, Antarctica – Part 1: The diurnal changes, The Cryosphere, 18, 4547–4565, https://doi.org/10.5194/tc-18-4547-2024, 2024.

Morris, E. M. and Cooper, J. D.: Density measurements in ice boreholes using neutron scattering, Journal of Glaciology, 49, 599–604, https://doi.org/10.3189/172756503781830403, 2003.

Mottram, R., Hansen, N., Kittel, C., Van Wessem, J. M., Agosta, C., Amory, C., Boberg, F., Van de Berg, W. J., Fettweis, X., Gossart, A., Van Lipzig, N. P. M., Van Meijgaard, E., Orr, A., Phillips, T., Webster, S., Simonsen, S. B., and Souverijns, N.: What is the surface mass balance of Antarctica? An intercomparison of regional climate model estimates, The Cryosphere, 15, 3751–3784, https://doi.org/10.5194/tc-15-3751-2021, 2021.

Noël, B., van Wessem, J. M., Wouters, B., Trusel, L., Lhermitte, S., and van den Broeke, M. R.: Higher Antarctic Ice Sheet accumulation and surface melt rates revealed at 2 km resolution, Nat Commun, 14, 7949, https://doi.org/10.1038/s41467-023-43584-6, 2023.

Oke, T. R.: Boundary layer climates, 2nd ed., Routledge, London, 464 pp., https://doi.org/10.4324/9780203407219, 1987.

https://doi.org/10.5194/egusphere-2026-2150
Preprint. Discussion started: 27 May 2026

Ollivier, I., Steen-Larsen, H. C., Stenni, B., Arnaud, L., Casado, M., Cauquoin, A., Dreossi, G., Genthon, C., Minster, B., Picard, G., Werner, M., and Landais, A.: Surface processes and drivers of the snow water stable isotopic composition at Dome C, East Antarctica – A multi-dataset and modelling analysis, The Cryosphere, 19, 173–200, https://doi.org/10.5194/tc-19-173-2025, 2025.

Otosaka, I. N., Shepherd, A., Ivins, E. R., Schlegel, N.-J., Amory, C., Van den Broeke, M. R., Horwath, M., Joughin, I., King, M. D., Krinner, G., Nowicki, S., Payne, A. J., Rignot, E., Scambos, T., Simon, K. M., Smith, B. E., Sørensen, L. S., Velicogna, I., Whitehouse, P. L., A, G., Agosta, C., Ahlstrøm, A. P., Blazquez, A., Colgan, W., Engdahl, M. E., Fettweis, X., Forsberg, R., Gallée, H., Gardner, A., Gilbert, L., Gourmelen, N., Groh, A., Gunter, B. C., Harig, C., Helm, V., Khan, S. A., Kittel, C., Konrad, H., Langen, P. L., Lecavalier, B. S., Liang, C.-C., Loomis, B. D., McMillan, M., Melini, D., Mernild, S. H., Mottram, R., Mouginot, J., Nilsson, J., Noël, B., Pattle, M. E., Peltier, W. R., Pie, N., Roca, M., Sasgen, I., Save, H. V., Seo, K.-W., Scheuchl, B., Schrama, E. J. O., Schröder, L., Simonsen, S. B., Slater, T., Spada, G., Sutterley, T. C., Vishwakarma, B. D., Van Wessem, J. M., Wiese, D., Van der Wal, W., and Wouters, B.: Mass balance of the Greenland and Antarctic Ice Sheets from 1992 to 2020, Earth System Science Data, 15, 1597–1616, https://doi.org/10.5194/essd-15-1597-2023, 2023.

Pritchard, H. D., Fretwell, P. T., Fremand, A. C., Bodart, J. A., Kirkham, J. D., Aitken, A., Bamber, J., Bell, R., Bianchi, C., Bingham, R. G., Blankenship, D. D., Casassa, G., Christianson, K., Conway, H., Corr, H. F. J., Cui, X., Damaske, D., Damm, V., Dorschel, B., Drews, R., Eagles, G., Eisen, O., Eisermann, H., Ferraccioli, F., Field, E., Forsberg, R., Franke, S., Goel, V., Gogineni, S. P., Greenbaum, J., Hills, B., Hindmarsh, R. C. A., Hoffman, A. O., Holschuh, N., Holt, J. W., Humbert, A., Jacobel, R. W., Jansen, D., Jenkins, A., Jokat, W., Jong, L., Jordan, T. A., King, E. C., Kohler, J., Krabill, W., Maton, J., Gillespie, M. K., Langley, K., Lee, J., Leitchenkov, G., Leuschen, C., Luyendyk, B., MacGregor, J. A., MacKie, E., Moholdt, G., Matsuoka, K., Morlighem, M., Mouginot, J., Nitsche, F. O., Nost, O. A., Paden, J., Pattyn, F., Popov, S., Rignot, E., Rippin, D. M., Rivera, A., Roberts, J. L., Ross, N., Ruppel, A., Schroeder, D. M., Siegert, M. J., Smith, A. M., Steinhage, D., Studinger, M., Sun, B., Tabacco, I., Tinto, K. J., Urbini, S., Vaughan, D. G., Wilson, D. S., Young, D. A., and Zirizzotti, A.: Bedmap3 updated ice bed, surface and thickness gridded datasets for Antarctica, Sci Data, 12, 414, https://doi.org/10.1038/s41597-025-04672-y, 2025.

Richter, A., Ekaykin, A. A., Willen, M. O., Lipenkov, V. Y., Groh, A., Popov, S. V., Scheinert, M., Horwath, M., and Dietrich, R.: Surface mass balance models vs. stake observations: A comparison in the Lake Vostok region, central East Antarctica, Front. Earth Sci., 9, 669977, https://doi.org/10.3389/feart.2021.669977, 2021.

Rignot, E., Mouginot, J., Scheuchl, B., van den Broeke, M., van Wessem, M. J., and Morlighem, M.: Four decades of Antarctic Ice Sheet mass balance from 1979–2017, Proceedings of the National Academy of Sciences, 116, 1095–1103, https://doi.org/10.1073/pnas.1812883116, 2019.

Roussel, M.-L., Lemonnier, F., Genthon, C., and Krinner, G.: Brief communication: Evaluating Antarctic precipitation in ERA5 and CMIP6 against CloudSat observations, The Cryosphere, 14, 2715–2727, https://doi.org/10.5194/tc-14-2715-2020, 2020.

Smith, B. E., Medley, B., Fettweis, X., Sutterley, T., Alexander, P., Porter, D., and Tedesco, M.: Evaluating Greenland surface-mass-balance and firn-densification data using ICESat-2 altimetry, The Cryosphere, 17, 789–808, https://doi.org/10.5194/tc-17-789-2023, 2023.

Sorge, E.: Glaziologische Untersuchungen in Eismitte, in K. Wegener: Wissenschaftliche Ergebnisse der Deutschen Grönlandexpedition Alfred Wegener 1929 und 1930/1931, F. A. Brockhaus, 3, 1935.

Stefanini, C., Stenni, B., Masiol, M., Dreossi, G., Favier, V., Becherini, F., Scarchilli, C., Ciardini, V., Carugati, G., and Frezzotti, M.: Challenges in surface mass balance estimation at Dome C: stake farm comparisons, measurement uncertainties, and station-induced biases, The Cryosphere, 19, 5781–5799, https://doi.org/10.5194/tc-19-5781-2025, 2025.

https://doi.org/10.5194/egusphere-2026-2150
Preprint. Discussion started: 27 May 2026

Stevens, C. M., Lilien, D. A., Conway, H., Fudge, T. J., Koutnik, M. R., and Waddington, E. D.: A new model of dry firn-densification constrained by continuous strain measurements near South Pole, Journal of Glaciology, 69, 2099–2113, https://doi.org/10.1017/jog.2023.87, 2023.

Takahashi, S. and Kameda, T.: Snow density for measuring surface mass balance using the stake method, Journal of Glaciology, 53, 677–680, https://doi.org/10.3189/002214307784409360, 2007.

Van Dalum, C., Van de Berg, W. J., Van den Broeke, M., and Hofsteenge, M.: Monthly RACMO2.4p1 data for Antarctica (11 km) for SMB, SEB and near-surface variables (1979-2025), Zenodo [data set], https://doi.org/10.5281/zenodo.19255213, 2026.

Van Dalum, C. T., Van de Berg, W. J., Gadde, S. N., Van Tiggelen, M., Van der Drift, T., Van Meijgaard, E., Van Ulft, L. H., and Van den Broeke, M. R.: First results of the polar regional climate model RACMO2.4, The Cryosphere, 18, 4065–4088, https://doi.org/10.5194/tc-18-4065-2024, 2024.

Van Dalum, C. T., Van de Berg, W. J., Van den Broeke, M. R., and Van Tiggelen, M.: The surface mass balance and near-surface climate of the Antarctic Ice Sheet in RACMO2.4p1, The Cryosphere, 19, 4061–4090, https://doi.org/10.5194/tc-19-4061-2025, 2025.

Van den Broeke, M. R., Reijmer, C. H., and Van de Wal, R. S. W.: A study of the surface mass balance in Dronning Maud Land, Antarctica, using automatic weather stations, Journal of Glaciology, 50, 565–582, https://doi.org/10.3189/172756504781829756, 2004.

Van Wessem, J. M., Van de Berg, W. J., Noël, B. P. Y., Van Meijgaard, E., Amory, C., Birnbaum, G., Jakobs, C. L., Krüger, K., Lenaerts, J. T. M., Lhermitte, S., Ligtenberg, S. R. M., Medley, B., Reijmer, C. H., Van Tricht, K., Trusel, L. D., Van Ulft, L. H., Wouters, B., Wuite, J., and Van den Broeke, M. R.: Modelling the climate and surface mass balance of polar ice sheets using RACMO2 – Part 2: Antarctica (1979–2016), The Cryosphere, 12, 1479–1498, https://doi.org/10.5194/tc-12-1479-2018, 2018.

Veldhuijsen, S. B. M., Van de Berg, W. J., Brils, M., Kuipers Munneke, P., and Van den Broeke, M. R.: Characteristics of the 1979–2020 Antarctic firn layer simulated with IMAU-FDM v1.2A, The Cryosphere, 17, 1675–1696, https://doi.org/10.5194/tc-17-1675-2023, 2023.

Verjans, V., Leeson, A. A., McMillan, M., Stevens, C. M., Van Wessem, J. M., Van de Berg, W. J., Van den Broeke, M. R., Kittel, C., Amory, C., Fettweis, X., Hansen, N., Boberg, F., and Mottram, R.: Uncertainty in East Antarctic firn thickness constrained using a model ensemble approach, Geophysical Research Letters, 48, e2020GL092060, https://doi.org/10.1029/2020GL092060, 2021.

Wang, Y., Ding, M., Reijmer, C. H., Smeets, P. C. J. P., Hou, S., and Xiao, C.: The AntSMB dataset: a comprehensive compilation of surface mass balance field observations over the Antarctic Ice Sheet, Earth System Science Data, 13, 3057–3074, https://doi.org/10.5194/essd-13-3057-2021, 2021.

Westhoff, J., Freitag, J., Orsi, A., Martinerie, P., Weikusat, I., Dyonisius, M., Faïn, X., Fourteau, K., and Blunier, T.: Combining traditional and novel techniques to increase our understanding of the lock-in depth of atmospheric gases in polar ice cores – Results from the EastGRIP region, The Cryosphere, 18, 4379–4397, https://doi.org/10.5194/tc-18-4379-2024, 2024.

Whitehouse, P. L., Bentley, M. J., Milne, G. A., King, M. A., and Thomas, I. D.: A new glacial isostatic adjustment model for Antarctica: calibrated and tested using observations of relative sea-level change and present-day uplift rates, Geophys J Int, 190, 1464–1482, https://doi.org/10.1111/j.1365-246X.2012.05557.x, 2012.

https://doi.org/10.5194/egusphere-2026-2150
Preprint. Discussion started: 27 May 2026

Xiao, C., Li, Y., Hou, S., Allison, I., Bian, L., and Ren, J.: Preliminary evidence indicating Dome A (Antarctica) satisfying preconditions for drilling the oldest ice core, Chin. Sci. Bull., 53, 102–106, https://doi.org/10.1007/s11434-007-0520-6, 2008a.

Xiao, C., Li, Y., Allison, I., Hou, S., Dreyfus, G., Barnola, J.-M., Ren, J., Bian, L., Zhang, S., and Kameda, T.: Surface characteristics at Dome A, Antarctica: first measurements and a guide to future ice-coring sites, Annals of Glaciology, 48, 82–87, https://doi.org/10.3189/172756408784700653, 2008b.

Yang, D., Ding, M., Zou, X., van den Broeke, M. R., van Tiggelen, M., Allison, I., Tian, B., Chen, X., and Xiao, C.: Surface energy balance and temperature inversion at Dome Argus, the summit of the East Antarctic Ice Sheet, Journal of Geophysical Research: Atmospheres, 130, e2025JD044304, https://doi.org/10.1029/2025JD044304, 2025.

Zhu, J., Xie, A., Qin, X., Wang, Y., Xu, B., and Wang, Y.: An assessment of ERA5 reanalysis for Antarctic near-surface air temperature, Atmosphere, 12, 217, https://doi.org/10.3390/atmos12020217, 2021.